

Course Reader

Lecture 2

Camera Models, Projective Geometry
and Colour Models

Introduction to Image Analysis
ARTORG Center for Biomedical Engineering Research
University of Bern

Spring 2026

*This reader covers all examinable material from Lecture 2.
Key definitions, derivations, and conceptual results are highlighted.*

Contents

| | | |
|-----------|--|-----------|
| 1 | Introduction: From Scene to Image | 2 |
| 2 | Camera Obscura and Historical Context | 2 |
| 3 | The Pinhole Camera Model | 2 |
| 3.1 | Core Geometry | 2 |
| 3.2 | Key Observations | 3 |
| 3.3 | Worked Example | 3 |
| 4 | Homogeneous Coordinates and the Camera Matrix | 3 |
| 4.1 | Why Homogeneous Coordinates? | 3 |
| 4.2 | Projection as Matrix Multiplication | 4 |
| 4.3 | The Full Camera Matrix | 4 |
| 4.4 | Intrinsic vs. Extrinsic Parameters | 4 |
| 4.5 | Why Homogeneous Coordinates Matter Algorithmically | 5 |
| 5 | Perspective Geometry and Vanishing Points | 5 |
| 5.1 | Why Parallel Lines Converge | 5 |
| 5.2 | Types of Perspective | 5 |
| 5.3 | The Horizon Line | 6 |
| 5.4 | Applications in Medical Imaging | 6 |
| 5.5 | Worked Example: Vanishing Point Computation | 6 |
| 6 | Lenses, Sensors, and the Imaging Pipeline | 6 |
| 6.1 | From Pinhole to Lens | 6 |
| 6.2 | Key Trade-offs Introduced by Lenses | 7 |
| 6.3 | Digital Sensors: CCD and CMOS | 7 |
| 6.4 | Bayer Pattern and Demosaicing | 7 |
| 7 | Human Vision and Colour Perception | 7 |
| 7.1 | Photoreceptors: Rods and Cones | 8 |
| 7.2 | Trichromatic Theory and Metamerism | 8 |
| 7.3 | Colour Blindness | 8 |
| 8 | Colour Spaces | 8 |
| 8.1 | RGB: The Additive Colour Model | 8 |
| 8.2 | HSV / HSI: Separating Colour from Brightness | 9 |
| 8.3 | CIE LAB: Perceptual Uniformity | 9 |
| 8.4 | CIE Chromaticity and Colour Gamuts | 10 |
| 8.5 | CMYK and YCbCr | 10 |
| 8.6 | Gamma Correction | 11 |
| 8.7 | White Balance | 11 |
| 9 | Choosing the Right Colour Space | 11 |
| 10 | Summary of Key Equations | 12 |
| 11 | Practice Questions | 12 |
| 12 | Recommended Reading | 13 |

1 Introduction: From Scene to Image

Every digital image is the end product of a chain of physical processes. Understanding that chain is essential for interpreting what algorithms see and for correcting the artifacts they encounter.

1. **Illumination.** A light source (sun, lamp, X-ray tube, fluorescence excitation laser) emits photons towards the scene.
2. **Interaction with matter.** Photons reflect off surfaces, scatter inside tissue, or pass through transparent media. The spectral composition and intensity of the outgoing light encode information about the scene.
3. **Optics.** The camera’s aperture and lens collect a subset of the outgoing photons and focus them onto the sensor plane. The optics determine the field-of-view, depth-of-field, and geometric distortions.
4. **Sensor.** A detector (CCD or CMOS photo-diode array) converts photon energy into electrical charge at each pixel site.
5. **Digitisation.** An analog-to-digital converter (ADC) maps the continuous voltage at each pixel site to a discrete integer value. The resulting 2D array of integers is the digital image.

This lecture focuses on step 3 (the geometric projection model) and on how colour—a property of light’s spectral content—is represented once the image reaches software.

2 Camera Obscura and Historical Context

The **camera obscura** (Latin: “dark chamber”) is the simplest imaging device and the direct ancestor of every photographic camera.

Principle. Light from an illuminated outdoor scene passes through a tiny hole in the wall of a darkened room. Because each ray travels in a straight line, an **inverted** image of the scene forms on the opposite wall.

History. The phenomenon was described by the Chinese philosopher Mozi (c. 400 BC) and systematically studied by Ibn al-Haytham (c. 1000 AD) in *Kitāb al-Manāẓir* (Book of Optics). Renaissance artists exploited the camera obscura for realistic drawing. Adding a lens to the aperture increases brightness (see Section 6), and adding a chemical or electronic sensor yields a camera.

The camera obscura motivates the *pinhole camera model*, the starting point for all projection geometry in computer vision.

3 The Pinhole Camera Model

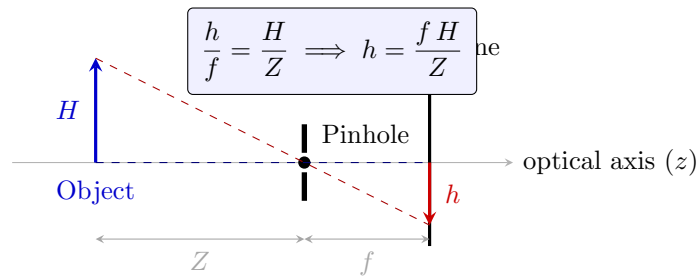
3.1 Core Geometry

Pinhole Camera Model

Place the camera centre (pinhole) at the origin. An image plane lies at distance f (the *focal length*) along the positive z -axis. A world point $\mathbf{P} = (X, Y, Z)^\top$ with $Z > 0$ projects to image coordinates:

$$x = f \frac{X}{Z}, \quad y = f \frac{Y}{Z} \quad (1)$$

This is the **virtual image plane** convention (image in front of the pinhole), which produces an upright image.



3.2 Key Observations

- **Non-linearity.** The mapping $(X, Y, Z) \mapsto (fX/Z, fY/Z)$ involves division by Z . This prevents us from writing it directly as a matrix–vector product in Euclidean coordinates.
- **Depth-dependent magnification.** Image size $h = fH/Z$: objects farther away (Z large) appear smaller.
- **Loss of depth.** All 3D points along a ray through the pinhole project to the *same* 2D point. Depth information is irrecoverably lost in a single view.
- **Inversion.** On the *real* image plane (behind the pinhole at $z = -f$), the image is inverted in both x and y (equivalent to a 180° rotation about the optical axis). The *virtual* image plane convention ($z = +f$) eliminates this negation—it is the standard in all computer-vision frameworks (OpenCV, PyTorch3D, etc.).

3.3 Worked Example

Example: Pinhole Projection

A building of height $H = 30$ m stands at distance $Z = 100$ m from a pinhole camera with $f = 50$ mm = 0.05 m.

Image height: $h = fH/Z = 0.05 \times 30/100 = 0.015$ m = 15 mm.

If the sensor has pixel pitch $5 \mu\text{m}$, the building spans $15 \text{ mm}/5 \mu\text{m} = 3000$ pixels.

4 Homogeneous Coordinates and the Camera Matrix

4.1 Why Homogeneous Coordinates?

The problem. The projection (1) is non-linear in (X, Y, Z) because of the $1/Z$ division. We cannot write it as $\mathbf{p} = M\mathbf{P}$ for any fixed matrix M .

The insight. If we represent both input and output in *homogeneous coordinates* and defer the final division, the projection becomes a **linear** map (matrix multiplication). The non-linearity is absorbed into a single, universal normalisation step.

Homogeneous Coordinates

- A 3D Euclidean point (X, Y, Z) is *lifted* to the 4-vector $\tilde{\mathbf{P}} = (X, Y, Z, 1)^\top \in \mathbb{P}^3$.
- A 2D image point (x, y) is represented as $\tilde{\mathbf{p}} = (x, y, 1)^\top$, or equivalently any non-zero scalar multiple $(kx, ky, k)^\top$.
- To **recover Euclidean coordinates**, divide by the last component:

$$(u, v, w)^\top \longrightarrow \left(\frac{u}{w}, \frac{v}{w} \right).$$

4.2 Projection as Matrix Multiplication

Choose $\lambda = Z$. Then:

$$Z \begin{pmatrix} x \\ y \\ 1 \end{pmatrix} = \begin{pmatrix} fX \\ fY \\ Z \end{pmatrix} = \underbrace{\begin{pmatrix} f & 0 & 0 \\ 0 & f & 0 \\ 0 & 0 & 1 \end{pmatrix}}_{\mathbf{K}_{\text{simple}}} \underbrace{\begin{pmatrix} 1 & 0 & 0 & 0 \\ 0 & 1 & 0 & 0 \\ 0 & 0 & 1 & 0 \end{pmatrix}}_{\Pi_0} \begin{pmatrix} X \\ Y \\ Z \\ 1 \end{pmatrix} \quad (2)$$

The entire right-hand side is a **matrix–vector product**—no division appears. The non-linearity is isolated in the final normalisation of the homogeneous output $(fX, fY, Z)^\top$ to the Euclidean point $(fX/Z, fY/Z)$.

The pipeline in three steps:

4.3 The Full Camera Matrix

Camera Projection Equation

$$\lambda \tilde{\mathbf{p}} = \mathbf{P} \tilde{\mathbf{X}} = \mathbf{K} [\mathbf{R} \mid \mathbf{t}] \tilde{\mathbf{X}} \quad (3)$$

where:

- $\mathbf{K} = \begin{bmatrix} f_x & s & c_x \\ 0 & f_y & c_y \\ 0 & 0 & 1 \end{bmatrix}$ is the 3×3 **intrinsic matrix**: focal lengths f_x, f_y (in pixels), principal point (c_x, c_y) , skew s (usually 0).
- $[\mathbf{R} \mid \mathbf{t}]$ is the 3×4 **extrinsic matrix**: rotation $\mathbf{R} \in \text{SO}(3)$ and translation $\mathbf{t} \in \mathbb{R}^3$ mapping world to camera coordinates.
- $\mathbf{P} = \mathbf{K}[\mathbf{R} \mid \mathbf{t}]$ is the 3×4 **camera matrix** (or projection matrix), with 11 degrees of freedom (a 3×4 matrix up to scale).

4.4 Intrinsic vs. Extrinsic Parameters

| Intrinsics \mathbf{K} (camera properties) | Extrinsics $[\mathbf{R} \mid \mathbf{t}]$ (camera pose) |
|---|---|
| Focal length(s) f_x, f_y | Rotation \mathbf{R} (3 angles: pitch, yaw, roll) |
| Principal point (c_x, c_y) | Translation $\mathbf{t} = (t_x, t_y, t_z)^\top$ |
| Pixel aspect ratio f_x/f_y | 6 degrees of freedom total |
| Skew s (usually 0) | |
| Fixed for a given camera/lens | Change with every new camera placement |
| Determined by <i>camera calibration</i> (checker-board) | Determined by <i>pose estimation</i> (PnP, SLAM, SfM) |

Practical Importance

Surgical navigation: Calibrate the endoscope (\mathbf{K}), then track its pose ($[\mathbf{R} \mid \mathbf{t}]$) in real-time to overlay surgical plans on the live video.

3D reconstruction: Both intrinsics and extrinsics are needed to triangulate 3D points from

2D correspondences in multiple views.

4.5 Why Homogeneous Coordinates Matter Algorithmically

- **Composition.** Multiple transforms (rotation, translation, intrinsics) are composed by matrix multiplication *before* being applied to any point—cheap and exact.
- **Batch efficiency.** A cloud of N points is projected by a single matrix product (a GPU-friendly operation).
- **Calibration.** Because the projection is linear in the entries of \mathbf{P} , camera calibration from 2D–3D correspondences reduces to a **linear least-squares** problem (Direct Linear Transform, DLT).
- **Projective geometry.** Many geometric relationships (collinearity, cross-ratio, homographies) have elegant linear forms in homogeneous coordinates that would require cumbersome case splits in Euclidean coordinates.

5 Perspective Geometry and Vanishing Points

5.1 Why Parallel Lines Converge

Under perspective projection, **3D parallel lines appear to converge** in the image. This is the most visible consequence of the $1/Z$ non-linearity.

Mathematical derivation. Consider two parallel rails at positions $(d_L, 0, t)$ and $(d_R, 0, t)$ for $t \in [0, \infty)$:

$$x_L = f \frac{d_L}{t}, \quad x_R = f \frac{d_R}{t}.$$

As $t \rightarrow \infty$, both $x_L \rightarrow 0$ and $x_R \rightarrow 0$. The two distinct 3D lines converge to the **same image point**: the **vanishing point**.

Vanishing Point

Lines parallel in 3D along direction $\mathbf{d} = (d_x, d_y, d_z)^\top$ converge in the image to:

$$\mathbf{v} = \mathbf{K} \begin{pmatrix} d_x/d_z \\ d_y/d_z \\ 1 \end{pmatrix} \quad (4)$$

The vanishing point depends only on the **direction** of the lines and the camera intrinsics, *not* on the lines' 3D positions.

5.2 Types of Perspective

- **One-point perspective.** One set of receding parallel lines \rightarrow one vanishing point (e.g., looking straight down a road).
- **Two-point perspective.** Two sets of parallels \rightarrow two VPs on the horizon (e.g., a building corner viewed at an angle).
- **Three-point perspective.** Three mutually orthogonal sets \rightarrow three VPs (e.g., looking up at a skyscraper—the vertical edges also converge).

The number of vanishing points visible in an image depends on how many distinct sets of parallel lines are present *and* on the camera orientation relative to those directions.

5.3 The Horizon Line

Horizon Line

The **horizon line** is the locus of *all* vanishing points for horizontal 3D directions. Key properties:

- When the camera is level, the horizon passes through the principal point (c_x, c_y) .
- Tilting the camera up shifts the horizon *down* in the image (and vice versa).
- The horizon's position encodes the camera's height and tilt angle.

5.4 Applications in Medical Imaging

Perspective geometry governs every optical modality:

- **Endoscopes:** Full perspective projection; understanding it is essential for 3D reconstruction from endoscopic video.
- **Optical microscopes:** At very small working depths relative to magnification, perspective effects are negligible → the **orthographic (parallel) projection** approximation is valid.
- **X-ray / CT:** Fan-beam or cone-beam geometry—a different projection model (not perspective but related).

5.5 Worked Example: Vanishing Point Computation

Example

Camera intrinsics:

$$\mathbf{K} = \begin{pmatrix} 500 & 0 & 320 \\ 0 & 500 & 240 \\ 0 & 0 & 1 \end{pmatrix}$$

. Lines are parallel along $\mathbf{d} = (1, 0, 2)^\top$.

Vanishing point:

$$\mathbf{v} = \begin{pmatrix} 500 & 0 & 320 \\ 0 & 500 & 240 \\ 0 & 0 & 1 \end{pmatrix} \begin{pmatrix} 1/2 \\ 0/2 \\ 1 \end{pmatrix} = \begin{pmatrix} 500 \cdot 0.5 + 320 \\ 500 \cdot 0 + 240 \\ 1 \end{pmatrix} = \begin{pmatrix} 570 \\ 240 \\ 1 \end{pmatrix}.$$

So the VP is at pixel $(570, 240)$ —to the right of the image centre, on the horizon.

Exam Tip — Vanishing Points

Be able to: (a) explain *why* parallel lines converge (cite the $1/Z$ factor); (b) compute a VP given \mathbf{K} and \mathbf{d} ; (c) distinguish one-, two-, and three-point perspective; (d) state what the horizon line is.

6 Lenses, Sensors, and the Imaging Pipeline

6.1 From Pinhole to Lens

A pinhole transmits too little light. Lenses focus light from each scene point onto a single sensor point, allowing a larger aperture.

Thin Lens Equation

$$\frac{1}{f} = \frac{1}{d_o} + \frac{1}{d_i} \quad (5)$$

f = focal length, d_o = object distance, d_i = image (sensor) distance.

6.2 Key Trade-offs Introduced by Lenses

- **Depth-of-field (DOF).** Only one depth is perfectly in focus. Out-of-focus points blur into a *circle of confusion*. A large aperture (small f -number) yields a **shallow** DOF; a small aperture yields a **deep** DOF but admits less light.
- **Aperture and f -number.** $N = f/D$ where D is the aperture diameter. $N = 1.4$ is “fast” (lots of light, shallow DOF); $N = 16$ is “slow” (less light, deep DOF).
- **Lens aberrations:**
 - *Spherical:* Rays through the lens edge focus at a different point than rays through the centre → edge blur.
 - *Chromatic:* Different wavelengths refract differently → colour fringing.
 - *Vignetting:* Light fall-off towards image corners.
 - *Distortion:* Barrel or pincushion bending of straight lines.

6.3 Digital Sensors: CCD and CMOS

Both CCD and CMOS sensors convert photons into electrons at each pixel site. The charge is then read out and digitised. Key differences:

| | CCD | CMOS |
|-----------------|-----------------------------|------------------------------|
| Readout | Sequential (shift register) | Per-pixel amplifier |
| Speed | Slower | Faster (row-parallel) |
| Noise | Lower (uniform readout) | Higher (fixed-pattern noise) |
| Power | Higher | Lower |
| Rolling shutter | No (global shutter) | Often yes |

6.4 Bayer Pattern and Demosaicing

Bayer Colour Filter Array

Each pixel records **one** colour channel through a colour filter. The standard **Bayer RGGB** pattern tiles 2×2 blocks: 50% green, 25% red, 25% blue—mirroring human cone sensitivity.

Demosaicing is the reconstruction of full RGB at every pixel site:

- **Bilinear:** Average neighbouring same-colour pixels. Fast, but may produce colour fringing at sharp edges.
- **Edge-directed:** Interpolate along detected edge directions rather than across them. Higher quality, higher cost.

7 Human Vision and Colour Perception

7.1 Photoreceptors: Rods and Cones

Photoreceptors

Rods ~120 million per eye. Extremely light-sensitive; responsible for **scotopic** (night) vision. No colour discrimination. Peak sensitivity ~507 nm.

Cones ~6 million per eye. Require bright light; responsible for **photopic** (day) vision and colour. Three types:

- **L-cones** (Long λ): peak ~560 nm (red/yellow), ~64% of cones.
- **M-cones** (Medium λ): peak ~530 nm (green), ~32% of cones.
- **S-cones** (Short λ): peak ~420 nm (blue/violet), ~2% of cones.

7.2 Trichromatic Theory and Metamerism

Young–Helmholtz trichromatic theory. The brain compares *ratios* of L, M, S cone activations to perceive colour. Any perceived colour is fully determined by a triple (l, m, s) of cone responses.

Metamerism

Two physically different light spectra $S_1(\lambda) \neq S_2(\lambda)$ that produce **identical** L, M, S cone responses are called **metamers**:

$$\int S_1(\lambda) \ell(\lambda) d\lambda = \int S_2(\lambda) \ell(\lambda) d\lambda, \quad (\text{and similarly for } m, s).$$

Metamerism is why **RGB displays work**: they need only match cone responses, not reproduce the full physical spectrum.

7.3 Colour Blindness

Missing or defective cones cause colour vision deficiencies (X-linked, affecting ~8% of males):

| Type | Missing cones | Prevalence (males) |
|------------|-----------------------|--------------------|
| Protanopia | L-cones (red-blind) | ~1% |
| Deutanopia | M-cones (green-blind) | ~1% |
| Tritanopia | S-cones (blue-blind) | Very rare |

Design implication: In medical imaging, avoid red-only or red-green-only colour maps. Use colourblind-safe palettes (viridis, Okabe–Ito).

8 Colour Spaces

8.1 RGB: The Additive Colour Model

RGB

A 3D cube with axes Red, Green, Blue:

- 8-bit: each channel $\in [0, 255]$; float: $\in [0, 1]$.
- Black $(0, 0, 0)$; White $(255, 255, 255)$; Red $(255, 0, 0)$.
- Additive mixing: $R + G = \text{Yellow}$, $G + B = \text{Cyan}$, $R + B = \text{Magenta}$, $R + G + B = \text{White}$.
- Grayscale conversion (Rec. 601): $L = 0.299R + 0.587G + 0.114B$.

Properties and limitations:

- **Device-dependent.** Same RGB triple looks different on different displays due to differing primaries and white points.
- **Not perceptually uniform.** Equal ΔRGB does *not* correspond to equal perceived colour difference.
- **High channel correlation** in natural images \rightarrow redundant for compression.

When to use: deep learning (CNNs), image I/O, display rendering, PNG/JPEG storage.

Exam Tip — BGR vs. RGB

OpenCV loads images in **BGR** channel order. Always convert with `cv2.cvtColor(img, cv2.COLOR_BGR2RGB)` before displaying with matplotlib or using libraries expecting RGB.

8.2 HSV / HSI: Separating Colour from Brightness

HSV Colour Space

Hue H Colour type; angle on colour wheel, 0° – 360° . Red $\approx 0^\circ$, Green $\approx 120^\circ$, Blue $\approx 240^\circ$.

Saturation S Purity: 0 (grey) to 1 (pure colour). $S = (V - \min(R, G, B))/V$.

Value V Brightness: 0 (black) to 1 (max brightness). $V = \max(R, G, B)$.

Geometry: a cylinder—hue is the angle, saturation is the radius, value is the height.

Advantages:

- **Hue is stable** under moderate illumination changes (V changes but H often does not).
- **Intuitive colour queries:** “find all red objects” \rightarrow threshold H near 0° .
- Cleanly separates chromatic from achromatic information.

Caveats:

- HSV is *not* perceptually uniform.
- Hue is undefined when $S = 0$ (achromatic).
- Hue wraps: red straddles 0° and 360° (in OpenCV: $H \in [0, 180]$, so red is near 0 *and* near 170–180).

When to use: colour-based segmentation (skin, tissue, dyes), object tracking, colour correction.

Case Study: Tissue Detection in Surgery

In endoscopic video, tissue hue is relatively stable ($H \approx 0^\circ$ – 25° in OpenCV’s 0–180 range). Saturation thresholds remove white drapes and dark shadows. Typical thresholds: $H \in [0, 20]$, $S \in [30, 255]$, $V \in [80, 255]$.

8.3 CIE LAB: Perceptual Uniformity

CIE LAB

L^* (**Lightness**) 0 (black) to 100 (white); non-linear mapping matching human brightness perception.

a^* Green (–) to Red (+) opponent axis; roughly -128 to $+127$.

b^* Blue (–) to Yellow (+) opponent axis; roughly -128 to $+127$.

Perceptual Colour Difference ΔE^*

$$\Delta E^* = \sqrt{(\Delta L^*)^2 + (\Delta a^*)^2 + (\Delta b^*)^2} \quad (6)$$

| ΔE^* | Perception |
|--------------|---------------------|
| < 1 | Imperceptible |
| ≈ 2 | Just noticeable |
| > 10 | Obviously different |

Equal Euclidean distances in $L^*a^*b^*$ \approx equal perceived colour differences.

Conversion chain:

$$\begin{pmatrix} X \\ Y \\ Z \end{pmatrix} = \mathbf{M} \begin{pmatrix} R_{\text{lin}} \\ G_{\text{lin}} \\ B_{\text{lin}} \end{pmatrix} \quad (\mathbf{M} \text{ depends on primaries \& white point; } R_{\text{lin}} \text{ is gamma-decoded}) \quad (7)$$

$$L^* = 116 f\left(\frac{Y}{Y_n}\right) - 16, \quad a^* = 500 \left[f\left(\frac{X}{X_n}\right) - f\left(\frac{Y}{Y_n}\right) \right], \quad b^* = 200 \left[f\left(\frac{Y}{Y_n}\right) - f\left(\frac{Z}{Z_n}\right) \right] \quad (8)$$

where $f(t) = t^{1/3}$ for $t > (6/29)^3$ and is linear otherwise. (X_n, Y_n, Z_n) is the reference white point.

Device-independent: Based on CIE XYZ tristimulus values modelling the physical human visual response, not any particular display.

When to use: measuring colour differences, stain normalisation in digital pathology, colour segmentation robust to illumination, display/print calibration.

8.4 CIE Chromaticity and Colour Gamuts

The **CIE xy chromaticity diagram** shows all colours visible to the human eye as a horseshoe-shaped region. Within it, colour spaces (sRGB, Adobe RGB, Rec. 2020) occupy triangular subregions called **gamuts**—the range of colours a device can reproduce.

Key facts:

- sRGB covers only $\sim 35\%$ of visible colours.
- Medical monitors may use wider gamuts (Display P3, Rec. 2020).
- A colour outside a device's gamut must be *gamut-mapped* (clipped or compressed) for display.

8.5 CMYK and YCbCr

| Space | Model | Key Properties |
|--------------|--|---|
| CMYK | Subtractive: Cyan, Magenta, Yellow, Key (Black). Inks <i>absorb</i> light. | Smaller gamut than RGB. K added because impure CMY inks yield brown, not black. Used in printing. |
| YCbCr | Y =luminance, C_b =blue-diff. chroma, C_r =red-diff. chroma. | Exploits lower human sensitivity to chroma detail. Chroma subsampling (4:2:0) saves $\sim 50\%$ bandwidth. Used in JPEG, H.264/H.265. |

Chroma subsampling: 4:4:4 (full), 4:2:2 (halve horizontal chroma), 4:2:0 (halve both dims—standard in JPEG and video).

8.6 Gamma Correction

Raw sensor output is **linear** w.r.t. photon count. Human vision is **non-linear** (Weber–Fechner law: sensitivity $\propto 1/\text{intensity}$).

Gamma Encoding

$$V_{\text{out}} = V_{\text{in}}^{1/\gamma}, \quad \gamma \approx 2.2 \text{ (sRGB)}. \quad (9)$$

Gamma encoding compresses bright values and expands dark values, producing a perceptually balanced allocation of bits.

Important rule: Always **gamma-decode** before any linear signal-processing operation (averaging, denoising, compositing). Failing to do so applies operations in a non-linear space and produces incorrect results.

8.7 White Balance

Different light sources have different colour temperatures (daylight ≈ 6500 K, tungsten ≈ 3000 K). The sensor records the illuminant colour cast; **white balance** corrects it by scaling R, G, B so that a white object appears white.

Common method: the **grey-world assumption**—the average scene colour should be neutral grey, so scale each channel so its mean equals the global mean.

Critical in pathology: stain colours must be reproducible across different scanners and sites; white-balance errors propagate into stain-normalisation algorithms.

9 Choosing the Right Colour Space

Exam Tip — Colour-Space Selection

There is no universally “best” colour space. Be ready to justify your choice:

| Space | Best for | Key property |
|-------|---------------------------------|-------------------------------|
| RGB | Deep learning, I/O, display | Device-native, simple |
| HSV | Colour segmentation, tracking | Separates hue from brightness |
| LAB | Colour measurement, stain norm. | Perceptually uniform |
| CMYK | Printing | Subtractive model |
| YCbCr | Compression (JPEG, video) | Luminance/chroma separation |

10 Summary of Key Equations

| Concept | Equation |
|----------------------|--|
| Pinhole projection | $x = f X/Z, \quad y = f Y/Z$ |
| Camera matrix | $\lambda \tilde{\mathbf{p}} = \mathbf{K}[\mathbf{R} \mid \mathbf{t}]\tilde{\mathbf{X}}$ |
| Intrinsic matrix | $\mathbf{K} = \begin{bmatrix} f_x & s & c_x \\ 0 & f_y & c_y \\ 0 & 0 & 1 \end{bmatrix}$ |
| Vanishing point | $\mathbf{v} = \mathbf{K}(d_x/d_z, d_y/d_z, 1)^\top$ |
| Thin lens equation | $1/f = 1/d_o + 1/d_i$ |
| Grayscale (Rec. 601) | $L = 0.299R + 0.587G + 0.114B$ |
| HSV value/saturation | $V = \max(R, G, B), \quad S = (V - \min)/V$ |
| CIE LAB ΔE^* | $\sqrt{(\Delta L^*)^2 + (\Delta a^*)^2 + (\Delta b^*)^2}$ |
| Gamma encoding | $V_{\text{out}} = V_{\text{in}}^{1/\gamma}, \quad \gamma \approx 2.2$ |

11 Practice Questions

Camera Models & Projective Geometry

1. A point $\mathbf{P} = (3, -1, 5)$ is projected through a pinhole camera with $f = 100$ px and principal point at the origin. What are the image coordinates?
2. Why is pinhole projection non-linear, and how do homogeneous coordinates resolve this?
3. Camera: $\mathbf{K} = \begin{pmatrix} 500 & 0 & 320 \\ 0 & 500 & 240 \\ 0 & 0 & 1 \end{pmatrix}$. Find the vanishing point for direction $\mathbf{d} = (1, 0, 2)^\top$.
4. Explain the difference between intrinsic and extrinsic parameters. Which change when you move the camera?
5. What is depth-of-field, and how does the aperture size affect it?
6. Describe the Bayer pattern. Why is there twice as much green as red or blue?
7. A building of height 20 m is at distance 80 m from a pinhole camera with $f = 35$ mm. How tall is the image on the sensor?

Colour Models

8. What is metamerism, and why does it enable RGB displays?
9. A pixel has RGB (200, 50, 50). Compute V and S in HSV.
10. Why is CIE LAB preferred over RGB for measuring colour differences? What does $\Delta E^* < 1$ mean?
11. Explain gamma correction. Why must you gamma-decode before linear operations?

12. Which colour space for: (a) endoscopic tissue segmentation by colour, (b) JPEG compression, (c) stain reproducibility measurement? Justify each.
13. What is chroma subsampling 4:2:0, and why does it not noticeably degrade image quality?
14. A pathology scanner at site A and one at site B produce different RGB values for the same tissue. Name two factors that could cause this and suggest a correction strategy.

12 Recommended Reading

- Szeliski, *Computer Vision: Algorithms and Applications* (2nd ed.), Chapter 2 (Image Formation).
- Gonzalez & Woods, *Digital Image Processing*, Chapter 6 (Colour Image Processing).
- Hartley & Zisserman, *Multiple View Geometry in Computer Vision*, Chapter 6 (Camera Models) [advanced].